A JOINT PERSPECTIVE OF PERIODICALLY EXCITED EFFICIENT NLMS ALGORITHM AND INVERSE CYCLIC CONVOLUTION

Stefan Kühl, Sebastian Nagel, Tobias Kabzinski, Christiane Antweiler, Peter Jax

Institute of Communication Systems (IKS), RWTH Aachen University, Germany
{*kuehl, nagel, kabzinski, antweiler, jax*}*@iks.rwth-aachen.de*

ABSTRACT

Research in static and time-variant system identification has brought up a broad variety of identification algorithms. In acoustics, e.g., static measurements of transfer functions are commonly conducted using *Inverse Cyclic Convolution* (ICC) with *Exponential Sweep* excitation. Identification and tracking of time-variant systems, however, often employ adaptive filter algorithms, such as the *Normalized Least Mean Square* (NLMS) algorithm. An interesting implementation variant is the so-called *Efficient NLMS* (eNLMS) algorithm for arbitrary periodic excitation. ICC and the eNLMS algorithm originate from different fields and have so far evolved independently. This paper bridges the gap using a theoretical analysis of both algorithms to prove that they can be transferred into each other. This understanding provides a joint perspective, such that know-how from both fields can be combined to further optimize the system identification process.

Index Terms— Adaptive Filters, Efficient NLMS Algorithm, Inverse Cyclic Convolution, Acoustic System Identification, Perfect Sequences

1. INTRODUCTION

The problem to identify a linear system has been studied for many decades and depending on the underlying application, many identification methods have been proposed and optimized. The most common one for acoustic measurements is the so-called *Inverse Cyclic Convolution* (ICC), which performs a block-wise deconvolution in the frequency domain. This method is commonly used for static acoustic measurements, e.g., of room impulse responses [1]. In this context, many improvements of the identification algorithm have been proposed, such as regularization or windowing. Also, the excitation signal has been optimized, taking into account the characteristics of the environment as well as the physical properties of the measurement equipment. As a result, so-called *Exponential Sweeps* [2–5] are applied in acoustics nowadays, comprising a high *Signal-to-Noise Ratio* (SNR), a low crest factor, and a certain robustness against non-linear distortions, e.g., induced by loudspeakers.

A different, but related field of interest are digital signal processing techniques for iterative system identification and tracking of time-variant linear systems. Example applications are *Acoustic Echo Cancellation* [6, 7] and *Active Noise Control* [8]. Typical adaptation algorithms are the *Normalized Least Mean Square* (NLMS) algorithm, the *Recursive Least Square* (RLS) algorithm [9, 10] or *Kalman Filtering* [11, 12], enabling an efficient identification in every time instant. Also, these algorithms have been improved over the last decades, e.g., by sophisticated control mechanisms like adaptive step-sizes, preprocessing of the input signals and complexity reduction [6, 10, 13].

In the context of fast measurements of time-variant linear systems, so-called *Periodic Perfect Sequences* (PPSEQ) [14] have been introduced as optimal excitation signals for the NLMS algorithm [15]. This allows to track system changes over time iteratively. An implementation variant of the NLMS algorithm that is highly efficient for block-wise processing has been proposed in [16].

One application of this method is the dynamic measurement of individual *Head-Related Transfer Functions* (HRTFs) with high spatial resolution [17, 18]. Originally, this task was regarded as a static measurement problem and treated with ICC and *Exponential Sweep* excitation [1, 3]. The different approaches, i.e., static and dynamic measurement methods, have been considered separately due to their different origins.

In [19], it has been shown that ICC, NLMS, and its variant [16] for a step-size $\mu = 1$ are mathematically equivalent for PPSEQ excitation. Furthermore, in [20], an efficient implementation of the NLMS algorithm also for non-PPSEQ excitation was presented, which is called *Efficient NLMS* (eNLMS). It provides the same tracking capabilities as a PPSEQ-excited NLMS algorithm.

The aim of this paper is to bridge the gap between both approaches by showing that the eNLMS algorithm and ICC are mathematically equivalent also for arbitrary periodic excitation signals and step-sizes. This provides a deeper understanding of the eNLMS algorithm. Furthermore, it opens a joint perspective on both algorithms, which opens the possibility to combine knowledge gained in both fields. For example, adaptive step-size control, common for NLMS algorithms, can be applied for ICC. *Exponential Sweeps*, a common excitation for acoustic measurements, or regularization methods can be used for tracking of time-variant systems with eNLMS.

The paper is structured as follows. First, the mathematical notation and properties of the involved operators and signals like PPSEQ are introduced in Sec. 1.1 and 1.2. In Sec. 2, ICC and the eNLMS algorithm from [20] are reviewed and analyzed. In Sec. 3, the algorithmic equivalence is shown and complexity figures are discussed.

1.1. Notation and Preliminary Considerations

We consider a linear system, described by an FIR filter with the impulse response coefficient vector at time instance n of length N given by

$$\mathbf{h}(n) = [h_0(n), h_1(n), \ldots, h_{N-1}(n)]^T, \tag{1}$$

with input $x(n)$ and output $d(n)$. Throughout this paper bold letters define vectors or matrices and $(\cdot)^T$ denotes the transpose operation. With the input vector

$$\mathbf{x}(n) = [x(n), x(n-1), \ldots, x(n-N+1)]^T \tag{2}$$

containing the last N values of the real-valued input sequence $x(n)$, the output sequence can be calculated via the inner product

$$d(n) = \mathbf{h}^T(n) \cdot \mathbf{x}(n). \tag{3}$$

The *Discrete Fourier Transform* (DFT) is defined for $\mathbf{x}(n)$, containing previous input samples in reverse order, as

$$X_\mu(n) = \sum_{k=0}^{N-1} \mathrm{e}^{-\mathrm{j}\frac{2\pi}{N}\mu k} x(n-k),\ \mu = 0, 1, \ldots, N-1 \tag{4}$$

with frequency bin index μ. The DFT can be written in vector notation as $\mathbf{X}(n) = [X_0(n), X_1(n), \ldots X_{N-1}(n)]^T$.
Introducing the $N \times N$ *Discrete Fourier Transform matrix* $\mathbf{F}$ with the elements

$$f_{\mu k} = \mathrm{e}^{-\mathrm{j}\frac{2\pi}{N}\mu k},\ 0 \le \mu, k \le N-1 \tag{5}$$

in the μ-th row and k-th column, it holds that $\mathbf{X}(n) = \mathbf{F}\mathbf{x}(n)$. With the $N \times N$ identity matrix $\mathbf{I} = [\mathbf{e}_0, \mathbf{e}_1, \ldots, \mathbf{e}_{N-1}]$, where $\mathbf{e}_i,\ i = 0, 1, \ldots, N-1$ denote the columns of $\mathbf{I}$, the DFT matrix $\mathbf{F}$ and its inverse $\mathbf{F}^{-1}$ can also be determined as

$$\mathbf{F} = \mathrm{DFT}\{\mathbf{I}\}, \qquad \mathbf{F}^{-1} = \mathrm{IDFT}\{\mathbf{I}\}, \tag{6}$$

where the operators $\mathrm{DFT}\{\cdot\}$ and $\mathrm{IDFT}\{\cdot\}$ denote the column-wise DFT and inverse DFT of a matrix. Also, the properties

$$\mathbf{F}^{-1} = \frac{1}{N}\mathbf{F}^* = \frac{1}{N}\mathbf{F}^H \tag{7}$$

hold, where $(\cdot)^{-1}$ denotes the matrix inverse, $(\cdot)^*$ the conjugate and $(\cdot)^H$ the hermitian of a matrix. Note that a complex conjugation of $\mathbf{F}$ corresponds to mirroring of the columns using the specific *mirroring matrix*

$$\bar{\mathbf{\Gamma}} = \left[\mathbf{e}_0, \mathbf{e}_{(N-1)}, \ldots, \mathbf{e}_1\right]. \tag{8}$$

Then, $\mathbf{F}^*$ can also be expressed as

$$\mathbf{F}^* = \mathbf{F}\bar{\mathbf{\Gamma}} \tag{9}$$

For real-valued signals, the complex conjugation in the frequency domain also corresponds to a mirroring operation in the *time domain*, as can be verified by

$$\bar{\mathbf{x}}(n) = \mathbf{F}^{-1}\left[\mathbf{F}\mathbf{x}(n)\right]^* = \bar{\mathbf{\Gamma}}\mathbf{x}(n) \tag{10}$$

with the mirrored sequence

$$\bar{\mathbf{x}}(n) = [x(n), x(n-N+1), \ldots, x(n-1)]^T. \tag{11}$$

Similarly, a cyclic shift of a vector by n_0 samples to the right can be expressed using the *time domain shifting matrix*

$$\breve{\mathbf{\Gamma}}(n_0) = \left[\mathbf{e}_{n_0 \bmod N}, \mathbf{e}_{(1+n_0) \bmod N}, \ldots, \mathbf{e}_{(N-1+n_0) \bmod N}\right],$$

such that the shifted vector $\breve{\mathbf{x}}_{n_0}(n)$ can be expressed by a matrix operation according to

$$\breve{\mathbf{x}}_{n_0}(n) = \breve{\mathbf{\Gamma}}(n_0)\mathbf{x}(n). \tag{12}$$

This cyclic shift can also be written as cyclic convolution of $\mathbf{x}(n)$ with the cyclically shifted unit impulse vector $\mathbf{e}_{n_0 \bmod N}$, since $\breve{\mathbf{\Gamma}}(n_0)$ is a circulant matrix. The cyclic convolution is calculated by an element-wise multiplication of the frequency domain vectors $\mathbf{F}\mathbf{e}_{n_0 \bmod N}$ and $\mathbf{F}\mathbf{x}(n)$. In this paper, the element-wise multiplication is expressed by turning one of the vectors into a diagonal matrix, as in

$$\mathbf{F}\breve{\mathbf{x}}_{n_0}(n) = \underbrace{\mathrm{diag}\{\mathbf{F}\mathbf{e}_{n_0 \bmod N}\}}_{\mathbf{\Lambda}(n_0)}\mathbf{F}\mathbf{x}(n), \tag{13}$$

where $\mathrm{diag}\{\cdot\}$ describes the operation of putting the elements of a vector onto the main diagonal of a square diagonal matrix. $\mathbf{\Lambda}(n_0)$ denotes a diagonal *frequency domain shifting matrix*. Accordingly, the cyclic shift can be expressed using either a *time* or a *frequency domain shifting matrix*

$$\mathbf{F}\breve{\mathbf{x}}_{n_0}(n) \overset{(13)}{=} \mathbf{\Lambda}(n_0)\mathbf{F}\mathbf{x}(n) \overset{(12)}{=} \mathbf{F}\breve{\mathbf{\Gamma}}(n_0)\mathbf{x}(n). \tag{14}$$

1.2. Periodic Perfect Sequences (PPSEQ)

As the eNLMS is based on properties of the PPSEQs (e.g., [14]), they will be reviewed briefly. A PPSEQ with period N is a signal $p(n)$ which has an impulse-like auto-correlation function

$$\varphi_{pp}(\lambda) = \sum_{n=0}^{N-1} p(n)p(n+\lambda) = \begin{cases} E_p & \text{for } \lambda \bmod N = 0 \\ 0 & \text{otherwise.} \end{cases} \tag{15}$$

Due to this property, for a given PPSEQ $p(n)$ only N different mutually orthogonal vectors $\mathbf{p}_0, \mathbf{p}_1, \ldots, \mathbf{p}_{N-1}$ of length N occur with

$$\mathbf{p}_{n \bmod N} = \mathbf{p}(n) = [p(n), p(n-1), \ldots, p(n-N+1)]^T. \tag{16}$$

Alternatively, employing a time domain shifting matrix, we obtain

$$\mathbf{p}(n) = \breve{\mathbf{\Gamma}}(n)\mathbf{p}_0. \tag{17}$$

Due to (15) all vectors have the same energy $\mathbf{p}^T(n)\mathbf{p}(n) = E_p, \forall\, n$ and an ideally flat magnitude spectrum. Thus, for the squared magnitude spectrum of a PPSEQ we obtain

$$\mathrm{diag}\{[\mathbf{F}\mathbf{p}(n)]^*\}\mathrm{diag}\{\mathbf{F}\mathbf{p}(n)\} = E_p \cdot \mathbf{I}, \tag{18}$$

where the multiplication of diagonal matrices is used to express the element-wise multiplication of the vectors. In order to obtain a real-valued signal, the phase of a PPSEQ has to be anti-symmetric, but apart from that it can be chosen arbitrarily. Therefore, several classes of PPSEQs exist, e.g., pseudo-random noise sequences like *Odd-Perfect Sequences* [21] and *Ipatov Sequences* [22] as well as *Perfect Sweeps* [23].

2. SYSTEM IDENTIFICATION METHODS

For the actual system identification, a system model like in Fig. 1 has to be considered.

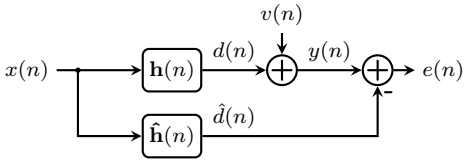

Fig. 1. Linear system with estimation path

The measured signal $y(n)$ comprises the desired output signal $d(n)$ as well as a disturbance signal $v(n)$. Both ICC and the eNLMS algorithm from [20] aim to estimate the true impulse response coefficient vector $\mathbf{h}(n)$ by $\hat{\mathbf{h}}(n)$ using only the known input sequence $x(n)$ and the measurable output $y(n)$.

2.1. Inverse Cyclic Convolution (ICC)

ICC estimates the impulse response coefficient vector via element-wise division of the DFT spectrum of the output sequence vector $\mathbf{y}(n) = [y(n), y(n-1), \ldots, y(n-N+1)]^T$ by that of the input sequence vector $\mathbf{x}(n)$, i.e.,

$$\hat{\mathbf{h}}_{\mathrm{ICC}}(n) = \mathbf{F}^{-1}\left[\mathrm{diag}\{\mathbf{F}\mathbf{x}(n)\}^{-1}\mathbf{F}\mathbf{y}(n)\right]^*. \tag{19}$$

The complex conjugation is required to compensate for the mirroring of the sequences $x(n)$ and $y(n)$ (cf. (10)). For the excitation signal, we have to ensure that $\mathbf{X}(n)$ does not have any zero entries, as otherwise the division cannot be performed. It should be noted that this is no major restriction because in typical measurement applications the excitation signal can be chosen accordingly.

2.2. Efficient NLMS Algorithm (eNLMS) [20]

To introduce the eNLMS algorithm, first an alternative system description of the true impulse response coefficient vector $\mathbf{h}(n)$ is considered. A transform domain is defined in which the true impulse response coefficient vector $\mathbf{h}(n)$ is represented by a transformed coefficient vector $\mathbf{c}(n) = [c_0(n), c_1(n), \ldots, c_{N-1}(n)]^T$. Second, the eNLMS algorithm is summarized. In the new transform domain, it works like a conventional NLMS algorithm, providing an estimate $\hat{\mathbf{c}}(n)$ for the transformed coefficients $\mathbf{c}(n)$. An inverse transform of $\hat{\mathbf{c}}(n)$ yields the desired impulse response vector estimate $\hat{\mathbf{h}}(n)$.

Alternative System Description

Following [20], every periodic sequence can be interpreted as the result of a cyclic convolution of a PPSEQ $p(n)$ of period N and a zero-phase sequence $\mathbf{s} = [s(0), s(1), \ldots, s(N-1)]^T$, which can be expressed in the frequency domain as

$$\mathbf{x}(n) = \mathbf{F}^{-1}\mathrm{diag}\{\mathbf{Fs}\}\mathbf{Fp}(n). \tag{20}$$

Note that the PPSEQ contributes the complete phase of $\mathbf{X}(n)$ and a constant scaling factor, whereas $\mathbf{S}$ only contributes to the magnitude spectrum. Furthermore, the zero-phase property results in a real spectrum $\mathbf{S}$ so that

$$[\mathbf{Fs}]^* = \mathbf{Fs}, \tag{21}$$

or equivalently $\bar{\mathbf{\Gamma}}\mathbf{s} = \mathbf{s}$. As in Sec. 2.1, we assume that $\mathbf{X}(n)$ has no zero components. Then, it is possible to find a zero-phase sequence $\mathbf{g} = [g(0), g(1), \ldots, g(N-1)]^T$ such that the cyclic convolution of $\mathbf{s}$ and $\mathbf{g}$ yields a unit impulse in the time domain or equivalently a flat magnitude spectrum in the frequency domain

$$\mathrm{diag}\{\mathbf{Fs}\}\mathrm{diag}\{\mathbf{Fg}\} = \mathbf{I}. \tag{22}$$

The sequence $\mathbf{g}$ is now used as a pre-equalization of the perfect sequence $\mathbf{p}_i$ by a cyclic convolution according to

$$\mathbf{w}_i = \frac{1}{E_p}\mathbf{F}^{-1}\mathrm{diag}\{\mathbf{Fg}\}\mathbf{Fp}_i, \quad i = 0, 1, \ldots, N-1. \tag{23}$$

The new vectors $\mathbf{w}_i$ define a non-orthogonal basis of $\mathbb{R}^N$ and, by construction, are orthogonal to $\mathbf{x}(n)$

$$\mathbf{x}_i^T\mathbf{w}_j = \begin{cases} 1 & \text{for } i = j \\ 0 & \text{otherwise.} \end{cases} \tag{24}$$

With the new basis vectors $\mathbf{w}_i$, the desired output of the system in Fig. 1 can be calculated as

$$\begin{aligned} d(n) \overset{(3)}{=} \sum_{i=0}^{N-1} h_i(n)x(n-i) &= \sum_{i=0}^{N-1} h_i(n)\mathbf{e}_i^T\mathbf{x}(n) \\ &= \sum_{i=0}^{N-1} c_i(n)\mathbf{w}_i^T\mathbf{x}(n) \end{aligned} \tag{25}$$

with the transformed filter coefficients $c_i(n),\ i = 0, 1, \ldots, N-1$. Using the vector $\mathbf{c}(n)$ of all transformed filter coefficients and taking into account (24), eq. (25) can be rewritten as

$$\begin{aligned} d(n) &= \mathbf{x}_{n \bmod N}^T \left[\mathbf{w}_0, \mathbf{w}_1, \ldots, \mathbf{w}_{N-1}\right] \mathbf{c}(n) \\ &= \mathbf{e}_{n \bmod N}^T\mathbf{c}(n) = c_{n \bmod N}(n). \end{aligned} \tag{26}$$

This means that $d(n)$ corresponds to one of the filter coefficients as premultiplying by $\mathbf{e}_{n \bmod N}^T$ extracts the $(n \bmod N)$-th coefficient of $\mathbf{c}(n)$. Introducing an orthogonal permutation matrix

$$\mathbf{\Gamma}(n) = \left[\mathbf{e}_{n \bmod N}, \mathbf{e}_{(n-1) \bmod N}, \ldots, \mathbf{e}_{(n-N+1) \bmod N}\right], \tag{27}$$

the vector $\mathbf{d}(n) = [d(n), d(n-1), \ldots, d(n-N+1)]^T$ containing the last N output values of the linear system, is given by

$$\mathbf{d}(n) = \mathbf{\Gamma}^T(n)\mathbf{c}(n). \tag{28}$$

Thus, using the orthogonality $\mathbf{\Gamma}^T(n)\mathbf{\Gamma}(n) = \mathbf{I}$ of the matrix,

$$\mathbf{c}(n) = \mathbf{\Gamma}(n)\mathbf{d}(n). \tag{29}$$

This corresponds to mirroring and subsequent cyclic shifting, i.e.,

$$\mathbf{\Gamma}(n) = \breve{\mathbf{\Gamma}}(n) \cdot \bar{\mathbf{\Gamma}}. \tag{30}$$

Therefore, the vector of the filter coefficients is a cyclically shifted version of the N previous output samples.

By comparing equation (3) and (25), the inverse transform can be expressed by

$$\mathbf{h}(n) = \sum_{i=0}^{N-1} c_i(n)\mathbf{w}_i \tag{31}$$

which describes a cyclic convolution of the basis vector $\mathbf{w}_0$ and the coefficient vector $\mathbf{c}(n)$ and can therefore be calculated in the frequency domain as

$$\mathbf{h}(n) = \mathbf{F}^{-1}\mathrm{diag}\{\mathbf{Fw}_0\}\mathbf{Fc}(n). \tag{32}$$

By inserting equation (29), the filter coefficients can be written as a function of the output samples $\mathbf{d}(n)$,

$$\mathbf{h}(n) = \mathbf{F}^{-1}\mathrm{diag}\{\mathbf{Fw}_0\}\mathbf{F\Gamma}(n)\mathbf{d}(n). \tag{33}$$

Adaptation Algorithm

The adaptation algorithm as described in [16, 20] estimates the transformed coefficients $\mathbf{c}(n)$ of the unknown system model applying the conventional NLMS adaptation

$$\hat{\mathbf{c}}(n+1) = \hat{\mathbf{c}}(n) + \mu\big(y(n) - \hat{\mathbf{c}}^T(n)\mathbf{e}_{n \bmod N}\big)\mathbf{e}_{n \bmod N} \tag{34}$$

onto the estimated transformed impulse response coefficients $\hat{\mathbf{c}}(n)$ with the scalar step-size μ. The transform domain is designed such that a unit vector $\mathbf{e}_{n \bmod N}$ appears as excitation vector. Thus, in every single time instant only one coefficient $c_i(n)$ is updated – key to the efficiency of the eNLMS algorithm. For the special case $\mu = 1$, (34) becomes $\hat{\mathbf{c}}(n) = \mathbf{\Gamma}(n)\mathbf{y}(n)$ and the inverse transform (32) yields the estimated impulse response vector

$$\hat{\mathbf{h}}_{\mathrm{NLMS}}^{\mu=1}(n) = \mathbf{F}^{-1}\mathrm{diag}\{\mathbf{Fw}_0\}\mathbf{F\Gamma}(n)\mathbf{y}(n). \tag{35}$$

3. PROOF OF EQUIVALENCE

To prove that the eNLMS algorithm and ICC are equivalent, we first conduct the proof for step-size $\mu = 1$. Then, we illustrate that the choice of a smaller step-size in the eNLMS algorithm leads to an averaging process which can also be applied to ICC. Eventually, we show that both methods exhibit similar computational complexity.

3.1. Equivalence for Step-Size $\mu = 1$

For $\mu = 1$, we must show the equality of $\hat{\mathbf{h}}_{\mathrm{NLMS}}^{\mu=1}(n)$ from (35) and $\hat{\mathbf{h}}_{\mathrm{ICC}}(n)$ from (19), i.e.,

$$\mathbf{F}^{-1}\mathrm{diag}\{\mathbf{F}\mathbf{w}_0\}\cdot\mathbf{F}\boldsymbol{\Gamma}(n)\mathbf{y}(n) \overset{!}{=} \mathbf{F}^{-1}\left[\mathrm{diag}\{\mathbf{F}\mathbf{x}(n)\}^{-1}\mathbf{F}\mathbf{y}(n)\right]^*.$$

Resolving the complex conjugation and premultiplying by $\mathbf{F}$ yields

$$\mathrm{diag}\{\mathbf{F}\mathbf{w}_0\}\cdot\mathbf{F}\boldsymbol{\Gamma}(n)\mathbf{y}(n) \overset{!}{=} \mathrm{diag}\{[\mathbf{F}\mathbf{x}(n)]^*\}^{-1}\mathbf{F}^*\mathbf{y}(n).$$

By multiplying with $\mathbf{F}\mathrm{diag}\{[\mathbf{F}\mathbf{x}(n)]^*\}$ from the left, we now need to show that

$$\mathbf{F}\underbrace{\mathrm{diag}\{[\mathbf{F}\mathbf{x}(n)]^*\}\mathrm{diag}\{\mathbf{F}\mathbf{w}_0\}}_{\text{(II)}}\cdot\underbrace{\mathbf{F}\boldsymbol{\Gamma}(n)}_{\text{(I)}}\mathbf{y}(n) \overset{!}{=} \mathbf{F}\mathbf{F}^*\mathbf{y}(n). \quad (36)$$

According to (30), we replace $\boldsymbol{\Gamma}(n)$ in (I). Then, we use the frequency domain definitions of mirroring (9) and cyclic shifting (14) to rewrite

$$\begin{aligned}\text{(I)} = \mathbf{F}\boldsymbol{\Gamma}(n) &\overset{(30)}{=} \mathbf{F}\check{\boldsymbol{\Gamma}}(n)\bar{\boldsymbol{\Gamma}}\\ &\overset{(14)}{=} \boldsymbol{\Lambda}(n)\mathbf{F}\bar{\boldsymbol{\Gamma}} \overset{(9)}{=} \boldsymbol{\Lambda}(n)\mathbf{F}^*. \end{aligned} \quad (37)$$

For (II), inserting the definitions of $\mathbf{x}(n)$ from (20) and $\mathbf{w}_0$ from (23) yields

$$\begin{aligned}\text{(II)} &= \mathrm{diag}\{[\mathbf{F}\mathbf{x}(n)]^*\}\mathrm{diag}\{\mathbf{F}\mathbf{w}_0\}\\ &\overset{(20)}{=}\mathrm{diag}\{[\mathbf{F}\mathbf{s}]^*\}\mathrm{diag}\{[\mathbf{F}\mathbf{p}(n)]^*\}\mathrm{diag}\{\mathbf{F}\mathbf{w}_0\}\\ &\overset{(23)}{=}\mathrm{diag}\{[\mathbf{F}\mathbf{s}]^*\}\mathrm{diag}\{[\mathbf{F}\mathbf{p}(n)]^*\}\mathrm{diag}\{\mathbf{F}\mathbf{g}\}\mathrm{diag}\{\frac{1}{E_p}\mathbf{F}\mathbf{p}_0\}.\end{aligned}$$

As the order of multiplying diagonal matrices does not matter, this can be rearranged and simplified using the zero-phase property (21) and the relationship between $\mathbf{s}$ and $\mathbf{g}$ as defined in (22) to

$$\begin{aligned}\text{(II)} &\overset{(21)}{=} \underbrace{\mathrm{diag}\{\mathbf{F}\mathbf{s}\}\mathrm{diag}\{\mathbf{F}\mathbf{g}\}}_{\overset{(22)}{=}\mathbf{I}}\mathrm{diag}\{[\mathbf{F}\mathbf{p}(n)]^*\}\mathrm{diag}\{\frac{1}{E_p}\mathbf{F}\mathbf{p}_0\}\\ &=\frac{1}{E_p}\mathrm{diag}\{[\mathbf{F}\mathbf{p}(n)]^*\}\mathrm{diag}\{\mathbf{F}\mathbf{p}_0\}.\end{aligned} \quad (38)$$

Note that in (38), the zero-phase component $\mathbf{s}$ has been compensated, such that only the PPSEQ component remains. Since $\mathbf{p}(n)$ is a shifted version of $\mathbf{p}_0$ according to (17), the frequency domain shifting matrix (14) can also be used for $\mathbf{F}\mathbf{p}(n)$:

$$\begin{aligned}\text{(II)} &\overset{(17)}{=} \frac{1}{E_p}\mathrm{diag}\{\left[\mathbf{F}\check{\boldsymbol{\Gamma}}(n)\mathbf{p}_0\right]^*\}\mathrm{diag}\{\mathbf{F}\mathbf{p}_0\}\\ &\overset{(14)}{=} \frac{1}{E_p}\mathrm{diag}\{[\boldsymbol{\Lambda}(n)\mathbf{F}\mathbf{p}_0]^*\}\mathrm{diag}\{\mathbf{F}\mathbf{p}_0\}\\ &= \boldsymbol{\Lambda}(-n)\frac{1}{E_p}\mathrm{diag}\{[\mathbf{F}\mathbf{p}_0]^*\}\mathrm{diag}\{\mathbf{F}\mathbf{p}_0\}.\end{aligned} \quad (39)$$

Inserting the frequency domain definition of the autocorrelation property of perfect sequences from (18) reveals that (II) describes a cyclic shift in the frequency domain, i.e.,

$$\text{(II)} \overset{(18)}{=} \boldsymbol{\Lambda}(-n)\frac{1}{E_p}E_p\cdot\mathbf{I} = \boldsymbol{\Lambda}(-n). \quad (40)$$

Inserting (I) $= \boldsymbol{\Lambda}(n)\mathbf{F}^*$ from (37) and (II) $= \boldsymbol{\Lambda}(-n)$ from (40) into (36) yields two cyclic shift operations compensating each other according to the definition of $\boldsymbol{\Lambda}(n)$ in (13), so that

$$\mathbf{F}\cdot\underbrace{\boldsymbol{\Lambda}(-n)\cdot\boldsymbol{\Lambda}(n)}_{=\mathbf{I}}\cdot\mathbf{F}^*\mathbf{y}(n) = \mathbf{F}\cdot\mathbf{F}^*\mathbf{y}(n) \quad (41)$$

completes the proof.

3.2. Arbitrary Step-Size

Inspecting (34), we observe that in every single time instant only one coefficient $c_i(n)$ is updated and thus, after N time instants each coefficient of $\hat{\mathbf{c}}$ has been updated exactly once. By applying (34) recursively $(N-1)$ times, the block-wise adaptation rule

$$\begin{aligned}\hat{\mathbf{c}}(n+N) &= \hat{\mathbf{c}}(n) + \mu(\boldsymbol{\Gamma}(n+N-1)\mathbf{y}(n+N-1) - \hat{\mathbf{c}}(n))\\ &= (1-\mu)\cdot\hat{\mathbf{c}}(n) + \mu\cdot(\boldsymbol{\Gamma}(n+N-1)\mathbf{y}(n+N-1))\end{aligned} \quad (42)$$

can be derived. This compact form is only achieved as in the transform domain unit vectors appear as excitation, which compose $\boldsymbol{\Gamma}(n+N-1)$. Inserting (42) in the inverse transform (32) yields

$$\begin{aligned}\hat{\mathbf{h}}(n+N) =&(1-\mu)\cdot\hat{\mathbf{h}}(n) + \mu\cdot\\ &\underbrace{\mathbf{F}^{-1}\mathrm{diag}\{\mathbf{F}\mathbf{w}_0\}\mathbf{F}\cdot\boldsymbol{\Gamma}(n+N-1)\mathbf{y}(n+N-1)}_{\hat{\mathbf{h}}_{\mathrm{NLMS}}^{\mu=1}(n+N)}.\end{aligned} \quad (43)$$

For $0 < \mu < 1$, (43) describes a block-wise recursive averaging process of the impulse response estimates $\hat{\mathbf{h}}_{\mathrm{NLMS}}^{\mu=1}(n+N)$. It is well understood that such an averaging allows to trade robustness against disturbances for tracking performance, which is desirable for many practical applications. As $\hat{\mathbf{h}}_{\mathrm{NLMS}}^{\mu=1}(n+N) = \hat{\mathbf{h}}_{\mathrm{ICC}}(n+N)$, the same averaging process can be applied to ICC with identical results.

3.3. Complexity

First, the complexity for $\mu = 1$ is considered by comparing (35) and (19). Both employ two DFT and one IDFT operations, which can be efficiently performed using the *Fast Fourier Transform* (FFT). The basis vector $\mathbf{w}_0$ in the eNLMS algorithm and the N possible input vectors $\mathbf{x}(n)$ in ICC are constant, so that the FFT thereof needs to be calculated and stored only once. Furthermore, in ICC the complex divisions in (19) can be replaced by complex multiplications if the inverse of the input spectra is stored. Since the complex conjugation in (19) compensates for the mirroring of $\mathbf{x}(n)$ and $\mathbf{y}(n)$, it can be omitted if the signals are stored in reverse order. The multiplication with $\boldsymbol{\Gamma}(n)$ in the eNLMS algorithm in (35) can be implemented likewise. Hence, both methods exhibit the same computational complexity, as N complex multiplications, one FFT, and one IFFT operation have to be performed for each identification step.

For the general case with $\mu \neq 1$, (34) can be interpreted as a recursive averaging of $\hat{\mathbf{c}}$. Therefore, one subtraction, addition, and multiplication are needed in each time instant. The same result can be achieved with ICC by averaging $\hat{\mathbf{h}}$ as shown in (43). Due to the linearity of the DFT and the periodicity of the input sequence, it can be shown that averaging $\hat{\mathbf{h}}$ reduces to averaging $\mathbf{y}$ (cf. (19)). Thus, the eNLMS algorithm and ICC exhibit the same computational complexity.

4. CONCLUSION

In this paper, we examined the *Efficient NLMS* algorithm (eNLMS, [20]) and *Inverse Cyclic Convolution* (ICC) for arbitrary periodic excitation. We have shown that both methods provide mathematically equal results and complexity figures. The presented analysis improves the understanding of the eNLMS algorithm and its interaction with non-PPSEQ input, e.g., *Exponential Sweeps*. The joint perspective on both methods and classes of excitation signals bridges the gap between ICC for static acoustic measurements and the eNLMS algorithm for dynamic tracking.

5. REFERENCES

[1] S. Müller and P. Massarani, "Transfer-function measurement with sweeps," *Journal of the Audio Engineering Society*, vol. 49, no. 6, pp. 443–471, 2001.

[2] A. Farina, "Advancements in impulse response measurements by sine sweeps," in *Audio Engineering Society Convention 122*, Vienna, Austria, May 2007.

[3] P. Majdak, P. Balazs, and B. Laback, "Multiple exponential sweep method for fast measurement of head-related transfer functions," *J. Audio Eng. Soc.*, vol. 55, no. 7/8, pp. 623–637, 2007.

[4] P. Majdak, P. Balazs, W. Kreuzer, and M. Dörfler, "A time-frequency method for increasing the signal-to-noise ratio in system identification with exponential sweeps," in *Proc. of IEEE International Conference on Acoustics, Speech and Signal Processing (ICASSP)*, Prague, Czech Republic, May 2011, pp. 3812–3815.

[5] P. Dietrich, B. Masiero, and M. Vorländer, "On the optimization of the multiple exponential sweep method," *J. Audio Eng. Soc.*, vol. 61, no. 3, pp. 113–124, 2013.

[6] J. Benesty, T. Gänsler, D.R. Morgan, M. Sondhi, and S.L. Gay, *Advances in Network and Acoustic Echo Cancellation*, Digital Signal Processing. Springer-Verlag, 2001.

[7] P. Vary and R. Martin, *Digital Speech Transmission: Enhancement, Coding and Error Concealment*, John Wiley & Sons, 2006.

[8] S. Elliott, *Signal Processing for Active Control*, Academic Press, 2000.

[9] S. Haykin, *Adaptive Filter Theory (2nd Ed.)*, Prentice-Hall, Inc., Upper Saddle River, NJ, USA, 1991.

[10] E. Hänsler and G. Schmidt, *Acoustic Echo and Noise Control – A Practical Approach*, John Wiley & Sons, 2004.

[11] G. Enzner and P. Vary, "Frequency-domain adaptive Kalman filter for acoustic echo control in hands-free telephones," *Signal Processing*, vol. 86, no. 6, pp. 1140–1156, 2006.

[12] C. Paleologu, J. Benesty, and S. Ciochină, "Study of the general Kalman filter for echo cancellation," *IEEE Transactions on Audio, Speech and Language Processing*, vol. 21, no. 8, pp. 1539–1549, Aug. 2013.

[13] S. Kühl, C. Antweiler, T. Hübschen, and P. Jax, "Kalman filter based system identification exploiting the decorrelation effects of linear prediction," in *Proc. of IEEE International Conference on Acoustics, Speech, and Signal Processing (ICASSP)*, New Orleans, LA, USA, Mar. 2017.

[14] H. D. Lüke, "Sequences and arrays with perfect periodic correlation," *IEEE Transactions on Aerospace and Electronic Systems*, vol. 24, no. 3, pp. 287–294, May 1988.

[15] C. Antweiler, A. Telle, P. Vary, and G. Enzner, "Perfect-sweep NLMS for time-variant acoustic system identification," in *Proc. of IEEE International Conference on Acoustics, Speech and Signal Processing (ICASSP)*, Kyoto, Japan, Mar. 2012, pp. 517–520.

[16] A. Carini, "Efficient NLMS and RLS algorithms for perfect periodic sequences," in *Proc. of IEEE International Conference on Acoustics, Speech and Signal Processing (ICASSP)*, Dallas, TX, USA, Mar. 2010, pp. 3746–3749.

[17] G. Enzner, "Analysis and optimal control of LMS-type adaptive filtering for continuous-azimuth acquisition of head related impulse responses," in *Proc. of IEEE International Conference on Acoustics, Speech, and Signal Processing (ICASSP)*, Las Vegas, NV, USA, Mar. 2008, pp. 393–396.

[18] G. Enzner, C. Antweiler, and S. Spors, "Trends in acquisition of individual head-related transfer functions," in *The Technology of Binaural Listening*, Jens Blauert, Ed., pp. 57–92. Springer, Berlin, Heidelberg, 2013.

[19] C. Antweiler, S. Kühl, B. Sauert, and P. Vary, "System identification with perfect sequence excitation – efficient NLMS vs. inverse cyclic convolution," in *ITG Fachtagung Speech Communication*, Erlangen, Germany, Sept. 2014.

[20] A. Carini, "Efficient NLMS and RLS algorithms for perfect and imperfect periodic sequences," *IEEE Transactions on Signal Processing*, vol. 58, no. 4, pp. 2048–2059, Apr. 2010.

[21] H. D. Lüke and H. D. Schotten, "Odd-perfect, almost binary correlation sequences," *IEEE Transactions on Aerospace and Electronic Systems*, vol. 31, no. 1, pp. 495–498, Jan. 1995.

[22] V. P. Ipatov, "Ternary sequences with ideal periodic autocorrelation properties," *Radio Engineering and Electronic Physics*, vol. 24, pp. 75–79, 1979.

[23] A. Telle, C. Antweiler, and P. Vary, "Der perfekte Sweep - Ein neues Anregungssignal zur adaptiven Systemidentifikation zeitvarianter akustischer Systeme," in *Proceedings of the German Annual Conference on Acoustics (DAGA)*, Berlin, Germany, Mar. 2010, pp. 341–342.